# Methylenecyclopropane−Boron Trifluoride van der Waals Complexes; an Infrared and DFT Study

**Wouter A. Herrebout, Roman Szostak,† and Benjamin J. van der Veken***

*Department of Chemistry, Universitair Centrum Antwerpen, Groenenborgerlaan 171, B-2020 Antwerpen, Belgium*

*Received: May 8, 2000; In Final Form: June 15, 2000*

The formation of weakly bound molecular complexes between methylenecyclopropane (MeCP) and $BF_3$ dissolved in liquid argon has been investigated using FTIR spectroscopy. Experimental evidence was found for the formation of a 1:1 complex in which the $BF_3$ moiety binds to the exocyclic C═C double bond, whereas at higher concentrations of $BF_3$, weak absorption bands due to MeCP·$(BF_3)_2$ were also observed. Using spectra recorded at different temperatures between 105 and 129 K, the complexation enthalpy for the 1:1 complex in liquid argon was determined to be −10.7(3) kJ mol$^{-1}$. Structural and spectral information on the complexes was obtained from density functional calculations at the B3LYP/6-311++G(d,p) level. Applying Free Energy Perturbation Monte Carlo calculations to account for the solvent influences and statistical thermodynamics to calculate the zero-point vibrational and thermal influences, the complexation energy for the 1:1 complex was estimated, from the experimental complexation enthalpy, to be −16.0(10) kJ mol$^{-1}$. This value is compared with the B3LYP/6-311++G(d,p) complexation energies and with single point energies calculated at the MP2 = full/aug-cc-PVTZ level.

## Introduction

Boron halides play an important role in catalyzing a number of chemical reactions, and it is believed that the catalytic action is initiated through the formation of a precursor complex involving the boron halide.[1−3] Only a limited number of such complexes have been investigated in some detail. Among these are the complexes of ethene and propene with boron trifluoride, which have recently been characterized in liquid argon solutions.[4] In both cases, the electron deficient boron atom was found to interact with the $\pi$ electrons of the carbon−carbon double bond. The complexation enthalpies for these complexes were determined to be −10.0(2) and −11.8(2) kJ mol$^{-1}$, respectively. In the similar complex with cyclopropane,[5] ab initio calculations predict that the boron atom is situated in the plane formed by the ring carbon atoms, the interaction occurring with the center of one of the carbon−carbon bonds. For this species, the complexation enthalpy in liquid argon is significantly lower, equaling −7.8(6) kJ mol$^{-1}$.

In methylenecyclopropane, $C_4H_6$, further abbreviated as MeCP, both types of nucleophilic complexation sites are present. Complexes of this compound with hydrogen halides have been studied using matrix isolation[6] and jet expansion microwave spectroscopy.[7−9] In all cases, the hydrogen halide molecule was found to be hydrogen bonded to the carbon−carbon double bond. Although these complexes were investigated under nonequilibrium conditions, the fact that no complexes with the pseudo-$\pi$ sites were found indicates that the $\pi$-site leads to significantly stronger complexes than the pseudo-$\pi$ sites. No complexes of methylenecyclopropane with the boron trihalides have been reported up to now, but the significantly different complexation enthalpies for the $\pi$ and pseudo-$\pi$ complexes reported above appear to suggest that with $BF_3$ also the complex in which the interaction takes place with the carbon−carbon double bond would dominate.

Information on the $BF_3$ complexes with MeCP is reported in this study. First we will discuss the results of DFT calculations, which confirm that several types of complexes can be formed and that the complex with the carbon−carbon double bond is predicted as the more stable. Subsequently, the infrared spectra of mixed solutions, using liquid argon as a solvent, of MeCP and $BF_3$ will be discussed. It will be shown that the formation of complexes of MeCP with 1 and 2 molecules of $BF_3$ has been detected and that the combination of DFT with spectral data leads to the conclusion that in both cases the interaction takes place via the carbon−carbon double bond of MeCP.

## Experimental Section

The samples of MeCP (Fluka 66765, stated purity > 99%) and $BF_3$ (Praxair) were purified immediately prior to use on a low temperature, low pressure fractionation column. In the vapor phase spectra of the purified compounds, no bands due to impurities could be detected. The argon was supplied by l'Air Liquide and had a stated purity of 99.9999%.

The spectra were recorded on a Bruker IFS 66v Fourier Transform spectrometer, using a Globar source in combination with a Ge/KBr beam splitter and a broadband MCT detector. The interferograms were averaged over 200 scans, Happ-Genzel apodized and Fourier transformed using a zero filling factor of 4, to yield spectra at a resolution of 0.5 cm$^{-1}$. In cryosolutions, infrared bandwidths in general are a few wavenumbers; for such sharp bands, maxima can be read with a reproducibility of a few tenths of a wavenumber. Therefore, where justified, the maxima will be specified to 0.1 cm$^{-1}$. Because of the significant temperature shift of the band maxima in cryosolutions,[10] the

* To whom correspondence should be addressed. E-mail: bvdveken@ruca.ua.ac.be. Fax: int-32−3-2180233.

† Permanent address: Department of Chemistry, University of Wrocław, F. Joliot-Curie 14, 50-383 Wrocław, Poland.

10.1021/jp001677b CCC: $19.00 © 2000 American Chemical Society
Published on Web 08/23/2000

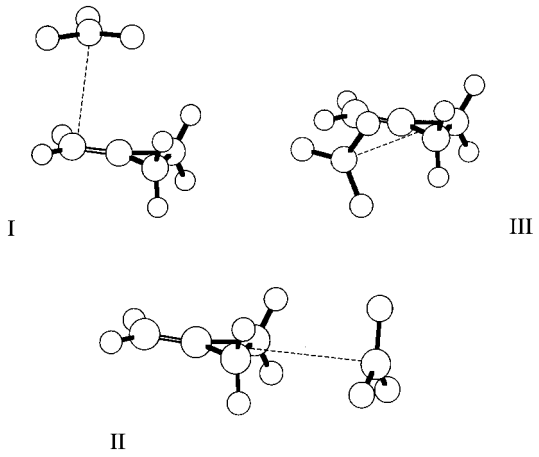


**Figure 1.** The stable isomers of MeCP·$BF_3$.

frequencies specified below were taken from spectra recorded at 110 K.

The experimental setup consists of a pressure manifold needed for filling and evacuating the cell and for monitoring the amount of gas used in a particular experiment, and the actual cell. The cell, with a path length of 7 cm, is equipped with slightly wedged, 5 mm thick Si windows, using a high-pressure window seal.[11] The cell can withstand an internal pressure of at least 150 bar at 77 K without leaking.

To be able to distinguish the spectra of undissolved species, spectra of amorphous and crystalline MeCP were recorded. The solids were obtained by condensing a small amount of the compound onto a CsI window, cooled to 10 K using a Leybold Heraeus ROK 10−300 cooling system, followed by annealing until no further changes were observed in the infrared spectrum.

### Computational Details

The density functional theory calculations were performed using Gaussian94.[12] For all calculations, Becke's three-parameter exchange functional[13] was used in combination with the Lee−Yang−Parr correlation functional,[14] whereas the 6-311++G-(d,p) basis set was used throughout as a compromise between accuracy and applicability to larger systems. To reduce the errors arising from the numerical integration, for all calculations the *finegrid* option, corresponding to roughly 7000 grid points per atom was used.

The complexation energies were calculated by subtracting the energies of the monomers from those of the complexes, and these energies were corrected for Basis Set Superposition Error using the counterpoise method of Boys and Bernardi.[15] For all equilibrium geometries, the vibrational frequencies and infrared intensities were calculated using standard harmonic force fields.

### Results

**A. DFT Calculations.** To gain insight into the structures and stabilities of the possible complexes between MeCP and $BF_3$, geometry optimizations were carried out starting from different relative positions of the molecules involved. These calculations converged to three minima, the equilibrium geometries of which are shown in Figure 1. The symmetry of complexes **I** and **II** is $C_s$, that of **III** is $C_1$. The complexation energies $\Delta E$, the Basis Set Superposition Errors $E_{BSSE}$ and the BSSE corrected complexation energies $\Delta E_{corr}$ for these complexes are collected in Table 1. The structural parameters of the different species can be evaluated from the Cartesian coordinates of the atoms in the equilibrium geometries that are listed in Table S1 of the Supplementary Information. Because of the large number of internal coordinates involved, no detailed description of the calculated equilibrium geometries will be given.

**TABLE 1. B3LYP/6-311++G(d,p) Interaction Energies, in kJ mol$^{-1}$, for the 1:1 Complexes Formed between MeCP, Ethene, Cyclopropane, and $BF_3$**

| | $\Delta E$ | $E_{BSSE}$ | $\Delta E_{corr}$ |
|---|---|---|---|
| MeCP·$BF_3$[a] | | | |
| **I** | −9.00 | 2.80 | −6.20 |
| **II** | −4.94 | 2.28 | −2.66 |
| **III** | −2.92 | 1.96 | −0.96 |
| $C_2H_4$·$BF_3$ | −6.94 | 2.44 | −4.70 |
| *c*-$C_3H_6$·$BF_3$ | −5.36 | 2.31 | −3.05 |

[a] The Roman numerals refer to the numbering of the isomers in Figure 1.

In the most stable isomer, **I**, $BF_3$ binds to the exocyclic C=C double bond, whereas in the stable structures **II** and **III**, the electron deficient B atom interacts with the $C_2-C_3$ and the $C_1-C_2$ bonds of the cyclopropyl ring. Obviously, the occurrence of these three stable isomers confirms that both the $\pi$ and pseudo-$\pi$ sites, in principle, can form complexes.

The calculated complexation energies suggest that the $\pi$-bonded complex **I** is significantly more stable than isomers **II** and **III**. If we treat, in a crude approximation, the BSSE corrected complexation energies as Gibbs energy differences at 110 K, a temperature typical for the experimental study, the populations for isomers **II** and **III** relative to that of the most stable isomer **I** are calculated to be 2 and 0.3%, respectively. Hence, it is not very likely that in cryosolutions the complexes **II** and **III** will be detected simultaneously with complex **I**. It will be seen below that this is confirmed by the experiments.

In Table 1, the calculated complexation energies for the $BF_3$ complexes with ethene and cyclopropane are also given. It can be seen that from $C_2H_4$·$BF_3$ to MeCP·$BF_3$ the complexation energy of the $\pi$ complex increases by 30%. In contrast, the complexation energies for isomers **II** and **III** are significantly smaller than that obtained for *c*-$C_3H_6$·$BF_3$.

The predicted vibrational frequencies and infrared intensities for monomers and complexes are summarized in Table 2. This table also contains the complexation shifts $\Delta\nu = \nu_{complex} - \nu_{monomer}$. Because of the relatively weak interactions between the monomers, the vibrations of the complexes can easily be subdivided into modes localized in the $BF_3$ or MeCP moieties and into intermolecular van der Waals modes. The latter are predicted to give rise to very weak bands in the far-infrared. This region was not investigated, and thus, only modes localized in MeCP and in $BF_3$ will be discussed here. The latter can unambiguously be correlated with the modes of the isolated monomers. Therefore, we will describe them using the assignments of the monomer vibrations. The Herzberg numbering scheme is used and the symbol is expanded with the formula of the monomer as a superscript. With one exception, the complexation shifts for MeCP depend very little on the boron isotope, the differences being well below 1 cm$^{-1}$. Therefore, in Table 2, only the results for the $^{11}B$ isotopomer are given. The exception is $\nu_5^{MeCP}$, for which the complexation shift in the $^{10}B$ isotopomer is +0.2 cm$^{-1}$ against −4.2 cm$^{-1}$ for the $^{11}B$ isotopomer. The reason for this is believed to be due to differences in the coupling of $\nu_5^{MeCP}$ with $\nu_3^{BF_3}$, which is present in the same spectral region. The complexation shifts in Table 2 will be discussed below, in relation to the experimental spectra.

It is generally accepted that van der Waals complexes are characterized by an extreme nonrigidity. To obtain information on this aspect for the present complexes, the barrier hindering

**TABLE 2. B3LYP/6-311++G(d,p) Vibrational Frequencies, in cm$^{-1}$, Infrared Intensities, in km mol$^{-1}$, and Complexation Shifts, in cm$^{-1}$, for the MeCP·BF$_3$ Complexes**

| | | | monomer | | complex **I** | | | complex **II** | | | complex **III** | | |
|---|---|---|---|---|---|---|---|---|---|---|---|---|---|
| mode | sym | description | $\nu$ | int | $\nu$ | int | $\Delta\nu$ | $\nu$ | int | $\Delta\nu$ | $\nu$ | int | $\Delta\nu$ |
| | | | | | | $^{11}BF_3$ modes | | | | | | | |
| $\nu_1$ | A$_1$′ | $^{11}BF_3$ stretch | 868.8 | 0.0 | 859.9 | 3.4 | −8.9 | 866.3 | 0.4 | -2.5 | 867.6 | 0.2 | -1.2 |
| $\nu_2$ | A$_2$′ | $^{11}BF$ bend | 681.9 | 102.2 | 638.2 | 220.9 | −43.7 | 665.3 | 185.8 | -16.6 | 673.5 | 151.9 | -8.4 |
| $\nu_3$ | E′ | $^{11}BF_3$ stretch | 1416.9 | 975.2 | 1410.2 | 399.5 | −6.7 | 1413.2 | 413.3 | -3.7 | 1414.7 | 418.2 | -2.2 |
| | | | | | 1397.4 | 355.2 | −19.5 | 1411.8 | 384.2 | -5.1 | 1412.0 | 377.3 | -4.9 |
| $\nu_4$ | E′ | $^{11}BF_3$ deform | 465.7 | 29.6 | 464.2 | 10.5 | −1.5 | 465.6 | 11.4 | -0.1 | 466.2 | 11.4 | 0.5 |
| | | | | | 463.5 | 9.6 | −2.2 | 464.8 | 11.5 | -0.9 | 464.7 | 12.3 | -1.0 |
| | | | | | | $^{10}BF_3$ modes | | | | | | | |
| $\nu_1$ | A$_1$′ | $^{10}BF_3$ stretch | 868.8 | 0.0 | 859.9 | 3.7 | −8.9 | 866.3 | 0.5 | -2.5 | 867.6 | 0.2 | -1.2 |
| $\nu_2$ | A$_2$′ | $^{10}BF$ bend | 709.7 | 110.7 | 663.6 | 241.0 | −46.1 | 691.1 | 201.0 | -18.6 | 700.9 | 165.1 | -8.8 |
| $\nu_3$ | E′ | $^{10}BF_3$ stretch | 1468.9 | 1067.6 | 1462.3 | 412.1 | −6.6 | 1465.2 | 437.4 | -3.7 | 1466.6 | 453.4 | -2.3 |
| | | | | | 1452.8 | 249.2 | −16.1 | 1464.8 | 428.1 | -4.1 | 1464.2 | 362.9 | -4.7 |
| $\nu_4$ | E′ | $^{10}BF_3$ deform | 467.5 | 28.8 | 466.1 | 10.2 | −1.4 | 467.5 | 11.1 | 0.0 | 468.1 | 11.1 | 0.6 |
| | | | | | 465.4 | 9.3 | −2.1 | 466.7 | 11.2 | -0.8 | 466.6 | 11.9 | -0.9 |
| | | | | | | MeCP modes[a] | | | | | | | |
| $\nu_1$ | A$_1$ | =CH$_2$ stretch | 3119.6 | 12.7 | 3119.5 | 7.8 | −0.1 | 3122.3 | 12.4 | 2.7 | 3124.0 | 10.1 | 4.4 |
| $\nu_2$ | A$_1$ | c-CH$_2$ stretch | 3100.6 | 13.7 | 3103.9 | 9.3 | 3.3 | 3098.6 | 10.3 | −2.0 | 3100.0 | 13.1 | −0.6 |
| $\nu_3$ | A$_1$ | C=C stretch | 1827.4 | 10.1 | 1817.8 | 13.9 | −9.6 | 1829.8 | 10.2 | 2.4 | 1825.0 | 9.0 | −2.4 |
| $\nu_4$ | A$_1$ | CH$_2$ scissors | 1482.0 | 0.1 | 1482.2 | 2.0 | 0.2 | 1481.2 | 0.1 | −0.8 | 1485.3 | 0.6 | 3.3 |
| $\nu_5$ | A$_1$ | CH$_2$ scissors | 1442.2 | 0.9 | 1442.8 | 1.8 | 0.6 | 1442.2 | 2.6 | 0.0 | 1446.2 | 1.4 | 4.0 |
| $\nu_6$ | A$_1$ | C−C stretch | 1060.0 | 3.7 | 1059.5 | 2.6 | −0.5 | 1053.5 | 9.4 | −6.5 | 1059.2 | 4.8 | -0.8 |
| $\nu_7$ | A$_1$ | c-CH$_2$ wag | 1029.3 | 4.4 | 1034.0 | 6.2 | 4.7 | 1039.5 | 1.5 | 10.2 | 1030.8 | 6.7 | 1.5 |
| $\nu_8$ | A$_1$ | C−C stretch | 737.5 | 6.3 | 736.0 | 5.4 | −1.5 | 735.4 | 0.6 | −2.1 | 736.2 | 5.3 | −1.3 |
| $\nu_9$ | A$_2$ | c-CH$_2$ stretch | 3170.9 | 0.0 | 3176.0 | 0.1 | 5.1 | 3171.5 | 0.0 | 0.6 | 3169.6 | 0.0 | −1.3 |
| $\nu_{10}$ | A$_2$ | c-CH$_2$ twist | 1162.3 | 0.0 | 1164.8 | 0.1 | 2.5 | 1166.5 | 0.0 | 4.2 | 1166.7 | 0.8 | 4.4 |
| $\nu_{11}$ | A$_2$ | CH$_2$ twist | 955.2 | 0.0 | 959.2 | 0.3 | 4.0 | 964.2 | 0.0 | 9.0 | 959.5 | 0.0 | 4.3 |
| $\nu_{12}$ | A$_2$ | CH$_2$ rock | 616.3 | 0.0 | 631.0 | 0.5 | 14.7 | 623.2 | 0.0 | 6.9 | 622.1 | 0.0 | 5.8 |
| $\nu_{13}$ | B$_1$ | c-CH$_2$ stretch | 3183.6 | 15.5 | 3188.3 | 10.0 | 4.7 | 3183.5 | 9.4 | −0.1 | 3182.6 | 11.8 | −1.0 |
| $\nu_{14}$ | B$_1$ | c-CH$_2$ twist | 1094.0 | 1.8 | 1097.9 | 2.5 | 3.9 | 1102.2 | 0.1 | 8.2 | 1095.0 | 2.2 | 1.0 |
| $\nu_{15}$ | B$_1$ | =CH$_2$ wag | 920.0 | 49.4 | 923.7 | 49.1 | 3.7 | 923.8 | 47.4 | 3.8 | 926.7 | 45.4 | 6.7 |
| $\nu_{16}$ | B$_1$ | c-CH$_2$ rock | 754.0 | 2.6 | 751.6 | 3.4 | −2.4 | 755.6 | 1.6 | 1.6 | 763.7 | 3.0 | 9.7 |
| $\nu_{17}$ | B$_1$ | C=CH$_2$ wag | 290.8 | 5.3 | 303.7 | 6.2 | 12.9 | 304.8 | 6.6 | 14.0 | 296.9 | 4.7 | 6.1 |
| $\nu_{18}$ | B$_2$ | =CH$_2$ stretch | 3199.7 | 11.8 | 3202.1 | 6.9 | 2.4 | 3203.3 | 10.3 | 3.6 | 3204.9 | 8.6 | 5.2 |
| $\nu_{19}$ | B$_2$ | c-CH$_2$ stretch | 3099.6 | 16.2 | 3102.9 | 10.7 | 3.3 | 3097.8 | 10.6 | −1.8 | 3095.6 | 12.3 | −4.0 |
| $\nu_{20}$ | B$_2$ | c-CH$_2$ scissors | 1446.8 | 2.8 | 1445.8 | 0.9 | −1.0 | 1447.8 | 12.4 | 1.0 | 1448.8 | 4.3 | 2.0 |
| $\nu_{21}$ | B$_2$ | =CH$_2$ rock | 1138.0 | 7.1 | 1141.5 | 6.8 | 3.5 | 1136.5 | 5.4 | −1.5 | 1138.2 | 8.1 | 0.2 |
| $\nu_{22}$ | B$_2$ | c-CH$_2$ wag | 1068.8 | 1.9 | 1072.6 | 1.2 | 3.8 | 1070.5 | 3.8 | 1.7 | 1075.3 | 2.9 | 6.5 |
| $\nu_{23}$ | B$_2$ | C−C stretch | 898.6 | 15.9 | 899.6 | 12.9 | 1.0 | 901.3 | 14.9 | 2.7 | 896.5 | 16.4 | −2.1 |
| $\nu_{24}$ | B$_2$ | C=CH$_2$ rock | 356.5 | 0.4 | 356.4 | 0.3 | −0.1 | 362.8 | 0.7 | 6.3 | 362.0 | 0.8 | 5.5 |
| | | | | | | Intermolecular modes | | | | | | | |
| | | | | | 85.6 | 1.2 | | 55.1 | 0.1 | | 60.0 | 0.0 | |
| | | | | | 83.8 | 0.1 | | 51.7 | 0.1 | | 37.8 | 0.1 | |
| | | | | | 74.2 | 1.8 | | 49.3 | 0.2 | | 37.0 | 0.1 | |
| | | | | | 62.2 | 0.0 | | 47.3 | 0.2 | | 36.8 | 0.1 | |
| | | | | | 45.0 | 0.0 | | 37.2 | 0.0 | | 31.0 | 0.0 | |
| | | | | | 15.6 | 0.0 | | 25.1 | 0.0 | | 7.8 | 0.0 | |

[a] For the MeCP·$^{11}$BF3 isotopomer.

rotation around the van der Waals bond was calculated for all isomers. For these calculations, the required angular parameter was systematically varied and at each value all other structural parameters were relaxed. The resulting barriers are 0.12 kJ mol$^{-1}$(**I**), 0.07 kJ mol$^{-1}$ (**II**) and 0.06 kJ mol$^{-1}$ (**III**). These barriers are significantly smaller than the value of $k_B$T in our experimental study and it follows that under the experimental conditions used, the complexes must be characterized by a large amplitude torsion. In this respect, the complexes between MeCP and $BF_3$ are not unlike other $BF_3$ complexes.[4]

**B. Vibrational Spectra.** The vibrational spectra of monomer $BF_3$ in liquid argon are well documented.[10] In contrast, no infrared data of MeCP in cryosolutions have been reported. To facilitate the description of the spectra, the characteristic frequencies for MeCP observed for a solution in LAr at 110 K, have been summarized in Table S2 of the Supporting Information. The assignments given are based on those reported for the vapor phase[16−19] and on the calculated frequencies summarized in Table 3.

In this study, infrared spectra of a series of mixtures in liquid argon, containing mole fractions of MeCP ranging from $1.7 \times 10^{-5}$ to $3.6 \times 10^{-4}$ and containing $BF_3$ with mole fractions between $6.0 \times 10^{-6}$ and $3.6 \times 10^{-4}$ were investigated. Apart from the monomer absorptions, new bands were observed in the spectra, which we assign to complexes formed between MeCP and $BF_3$. The frequencies of these bands, and their proposed assignment, are given in Table 3.

**$BF_3$ Modes.** The DFT results in Table 2 show that the vibrational frequencies of $BF_3$ are significantly disturbed by the complexation, the largest effect being calculated for $\nu_3^{BF_3}$. This region of the spectra is shown in Figure 2 for a solution in which the mole fractions of $BF_3$ and MeCP are $6.0 \times 10^{-6}$ and $2.4 \times 10^{-4}$, respectively. Two new bands, with maxima at 638.4 and 663.4 cm$^{-1}$, become prominently visible at lower temperatures.

**TABLE 3. Observed Vibrational Frequencies, in cm$^{-1}$, and Complexation Shifts, in cm$^{-1}$, for MeCP·BF$_3$ in Liquid Argon at 110 K**

| | monomer | | complex | |
|---|---|---|---|---|
| mode | $\nu$ | int | $\nu$ | $\Delta\nu$ |
| | | $^{11}BF_3$ modes | | |
| $\nu_1$ | 880.0[b] | n | 875.4 | −4.6 |
| $\nu_2$ | 680.9 | s | 638.4 | −42.5 |
| $\nu_3$ | 1444.8 | vs | 1435.0 | −9.8 |
| | | | 1429.5 | −15.3 |
| $\nu_4$ | 477.3 | w | 476.3 | −1.0 |
| $\nu_1+\nu_3$ | 2326.0 | s | 2306.9 | −19.1 |
| | | $^{10}BF_3$ modes | | |
| $\nu_2$ | 708.6 | s | 663.4 | −45.2 |
| $\nu_3$ | 1495.9 | vs | 1486.7 | −9.2 |
| | | | 1481.8 | −14.1 |
| $\nu_1+\nu_3$ | 2375.4 | s | 2356.2 | −19.2 |
| | | MeCP modes | | |
| $\nu_1$ | 3006.1 | s | 3004.9 | −1.2 |
| $\nu_3$ | 1739.6 | s | 1738.5 | −1.1 |
| $\nu_4$ | 1435.8 | w | 1438.7 | 2.9 |
| $\nu_5$ | 1408.3 | m | 1408.5 | 0.2 |
| $\nu_6$ | 1032.5 | s | 1034.8 | 2.3 |
| $\nu_7$ | 1001.8 | s | 1005.8 | 4.0 |
| $\nu_8$ | 724.3 | s | 724.3 | 0.0 |
| $\nu_{13}$ | 3067.6 | s | 3072.8 | 5.2 |
| $\nu_{14}$ | 1071.4 | m | 1075.5 | 4.1 |
| $\nu_{15}$ | 888.0 | vs | 901.9 | 13.9 |
| $\nu_{16}$ | 748.5 | m | 746.1 | −2.4 |
| $\nu_{18}$ | 3083.5 | s | 3083.2 | −0.3 |
| $\nu_{19}$ | 2995.1 | s | 2999.9 | 4.8 |
| $\nu_{20}$ | 1411.7 | m | 1412.2 | 0.5 |
| $\nu_{21}$ | 1123.1 | s | 1126.5 | 3.4 |
| $\nu_{22}$ | 1044.9 | m | 1048.0 | 3.1 |
| $\nu_{23}$ | 894.2 | s | 891.7 | −2.5 |
| $\nu_4+\nu_{21}$ | 2546.3 | vw | 2549.6 | 3.3 |
| $2\nu_{21}$ | 2242.8 | w | 2249.2 | 6.4 |
| $\nu_{21}+\nu_{22}$ | 2166.6 | vw | 2172.9 | 6.3 |
| $\nu_7+\nu_{21}$ | 2124.3 | vw | 2131.6 | 7.3 |
| $2\nu_{22}$ | 2084.8 | w | 2090.7 | 5.9 |
| $\nu_6+\nu_{22}$ | 2073.6 | w | 2079.1 | 5.5 |
| $\nu_7+\nu_{22}$ | 2039.6 | w | 2046.3 | 6.7 |
| $2\nu_7$ | 1975.7 | vw | 1983.3 | 7.6 |
| $2\nu_{15}$ | 1777.6 | s | 1794.6 | 17.0 |
| $\nu_8+\nu_{22}$ | 1764.8 | w | 1767.9 | 3.1 |
| $\nu_{22}+\nu_{24}$ | 1393.8 | w | 1395.3 | +1.5 |

[a] Abbreviations: vs very strong, s strong, m medium, w weak, vw very weak, n not active in IR spectrum. [b] From liquid-phase Raman spectrum, R. G. Steinhardt, G. E. S. Fetsch, M. W. Jordan, *J. Chem. Phys.* **1965**, *43*, 4528.

Assigning these as the $\nu_3^{BF_3}$ in the respective isotopomers of a 1:1 complex between MeCP and $BF_3$, they are found to be shifted by −42.2 and −45.2 cm$^{-1}$ from their respective monomer bands. Comparison with the data in Table 2 shows that these shifts are much larger than the values predicted for isomer **II**, −17 and −19 cm$^{-1}$, and those for isomer **III**, −8 and −9 cm$^{-1}$, but they agree very well with those predicted for isomer **I**, −44 and −46 cm$^{-1}$. In general, DFT complexation shifts that have been calculated for isolated species tend to reproduce the shifts observed in the inert cryosolutions rather well.[20] Therefore, the above result suggests the conclusion that in our solutions, isomer **I** is being formed. Moreover, the absence of other complex bands in this region also suggests that the concentrations of isomers **II** and **III** are below the detection limits of our experiments. In view of the very good signal-to-noise ratio in our spectra, and given that its complexation shift is nonzero, complex bands with a relative intensity of 1% of the corresponding monomer band should be easily detectable. As the DFT calculations do not suggest that the infrared intensities of the complex bands differ greatly from their monomer counterparts, it follows that the concentration of complexes **II** and **III** are well below 1% of that of the monomers. It will be shown in the following paragraphs that these conclusions are corroborated by the complex bands observed for other vibrational modes, both in $BF_3$ and in MeCP.

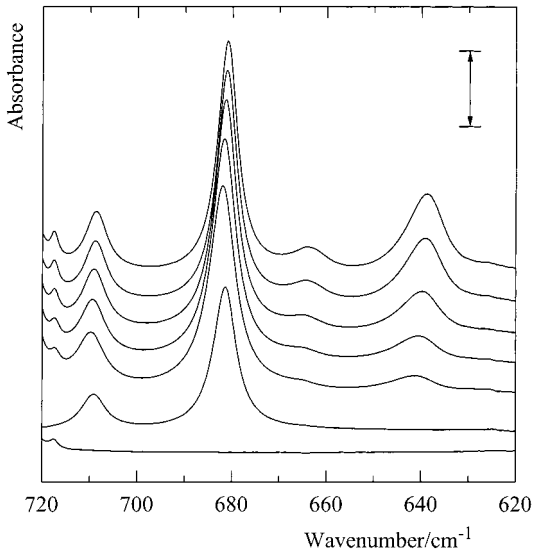


**Figure 2.** Infrared spectra of solutions in liquid argon in the region of $\nu_2^{BF_3}$. Top five traces: mixture of MeCP and $BF_3$; from top to bottom the temperature increases from 109 to 128 K. The lower two spectra are recorded at 109 K from solutions containing only $BF_3$ and MeCP, respectively. The length of the vertical double arrow corresponds to an absorbance of 0.25.

In all isomers of the 1:1 complex, the symmetry is lower than for monomer $BF_3$. As a consequence, the 2-fold degeneracy of $\nu_3^{BF_3}$ and $\nu_4^{BF_3}$ is lifted. Table 2 shows that especially for $\nu_3^{BF_3}$ significant splittings of the two components of the degenerate monomer mode are predicted, with clear differences for the different isomers. The region of $\nu_3^{BF_3}$ is shown in Figure 3. The upper trace is the experimental spectrum of a mixed solution, and the lower trace is the spectrum of monomer MeCP, rescaled such that it matches the monomer contributions to the upper trace. The out-of-scale bands at 1496 and 1445 cm$^{-1}$ in the upper trace are the monomer $\nu_3^{BF_3}$ bands in the $^{10}B$ and $^{11}B$ isotopomers, respectively. We assign the doublet with components at, approximately, 1487 and 1482 cm$^{-1}$ as $\nu_3^{BF_3}$ in the $^{10}B$ containing complex. The situation on the low-frequency side of the $^{11}B$ $\nu_3^{BF_3}$ is complicated by the presence of monomer MeCP bands, and, consequently, by their corresponding complex bands. To simplify matters, the monomer MeCP contributions were subtracted out, using the rescaled spectrum shown in the bottom trace of Figure 3. The rescaling factor was derived using the $2\nu_{15}^{MeCP}$ band at 1778 cm$^{-1}$. The complex band for the latter mode appears at 1795 cm$^{-1}$ and does not influence the band area of the monomer band. The rescaling factor was chosen such that in the difference spectrum, the 1778 cm$^{-1}$ band was completely canceled out. Because of the dilute nature of the solutions, it was accepted that the relative infrared intensities of MeCP in the monomer solution are the same as in the mixed solution, so that in the difference spectrum the other bands due to monomer MeCP canceled out to the same extent. The region of the difference spectrum appropriate for $\nu_3^{BF_3}$ is shown as the middle trace in Figure 3. In this, apart from three weak complex bands below 1420 cm$^{-1}$, obviously associated with MeCP modes, complex bands can be observed at 1439, 1435 and 1429.5 cm$^{-1}$. One of these must be associated with $\nu_4^{MeCP}$,

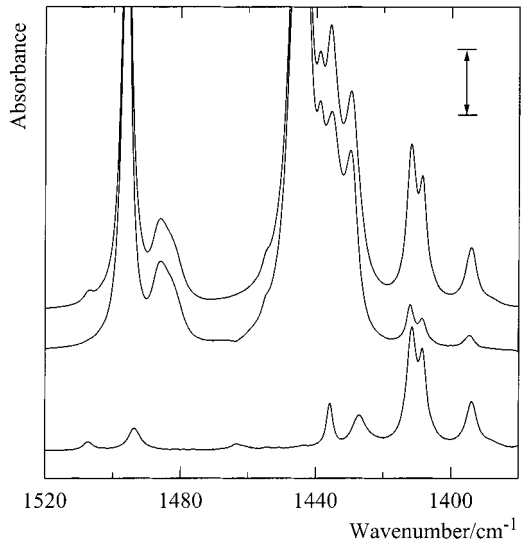


**Figure 3.** Infrared spectra of solutions in liquid argon in the region of $\nu_3^{BF_3}$, recorded at 106 K. Top trace: mixture of MeCP and $BF_3$; bottom trace: rescaled spectrum of a solution containing only MeCP; middle trace: difference spectrum resulting from the subtraction of the lower from the top trace. The length of the vertical double arrow corresponds to an absorbance of 0.25.

observed at 1436 $cm^{-1}$ in monomer MeCP. This mode is relatively weak, so that we prefer to associate the weaker of the three complex bands, at 1438 $cm^{-1}$, with this mode. Thus, the 1435 and 1429.5 $cm^{-1}$ bands are the $\nu_3^{BF_3}$ of the complex. Hence, for both isotopomers, this mode is split into a doublet, with a separation of 5.5 $cm^{-1}$ for the $^{11}B$ isotopomer. Table 2 shows that this separation is predicted at 12.8 $cm^{-1}$ for isomer **I**, and at 1.4 and 2.7 $cm^{-1}$ for isomers **II** and **III**, respectively; the observed splitting falls between the highest and lowest of the predicted values. Therefore, although their splitting confirms the lower symmetry of the complex, these doublets do not give straightforward information on the nature of the observed complex.

Finally, as a consequence of the lower symmetry of the complexes, the forbidden monomer mode $\nu_1^{BF_3}$ becomes weakly active, as reflected by the infrared intensities in Table 2. In the temperature-dependent study shown in Figure 5 (vide infra) this transition can be seen to grow in at lower temperatures, near 875 $cm^{-1}$.

**MeCP Modes.** Also, for modes localized in the MeCP moiety, complex bands were observed, as is illustrated in Figures 4−6. Figure 4 contains the details of a mixed solution containing mole fractions of $3.6 \times 10^{-4}$ in $BF_3$ and $1.2 \times 10^{-4}$ of MeCP. The region of the *c*-$CH_2$ rocking vibration $\nu_{16}^{MeCP}$ is shown in Figure 4A. The DFT frequencies in Table 2 indicate that in isomers **II** and **III** this mode should shift to higher frequencies, by 1.6 and 6.7 $cm^{-1}$, respectively, whereas in isomer **I,** it should shift in the opposite direction, by −2.4 $cm^{-1}$. Figure 4A shows that for the mixed solution, a single complex band occurs, shifted by approximately −2.4 $cm^{-1}$ and that no complex bands can be detected on the high frequency side of the monomer band. This clearly supports the above conclusion that in the cryosolutions studied, only isomer **I** is formed in measurable concentrations.

In Figure 4 also the regions of $\nu_7^{MeCP}$, $\nu_{14}^{MeCP}$ and $\nu_{21}^{MeCP}$ are given. Each of these modes appears to be well separated from the other bands in the monomer spectra, and for each, a complex band is present in the spectra of the mixed solution. Comparison with the DFT frequencies in Table 2 shows that the observed blue shift for $\nu_{21}^{MeCP}$ compares favorably with the predictions for isomer **I**, whereas it disagrees with the shifts for **II** and **III**. For the *c*-$CH_2$ wagging $\nu_7^{MeCP}$ and the *c*-$CH_2$ twisting $\nu_{14}^{MeCP}$, the DFT calculations predict blue shifts for all isomers. In agreement with this, in Figure 4, parts B and C, blue-shifted complex bands are observed. The experimental shifts, +4.0 and +3.9 $cm^{-1}$, agree much more closely with the predictions for isomer **I**, +4.7 and +3.9 $cm^{-1}$, than with those for the other isomers. This supports the identificiation of the complex as isomer **I**.

At the lowest temperatures, a weak feature emerges near 1079 $cm^{-1}$ in the spectra in Figure 4C. It is tempting to assign this band to isomer **II**, which, according to the DFT calculations, should appear at 8.2 $cm^{-1}$ above the 1071.4 $cm^{-1}$ monomer band. Because no other bands due to isomer **II** were observed, we prefer, however, to assign this band to a complex with higher stoichiometry, involving one MeCP molecule and two $BF_3$ molecules. We will return to this in a later paragraph.

In Figure 5 the region of the $=CH_2$ wagging $\nu_{15}^{MeCP}$ and the CC stretching $\nu_{23}^{MeCP}$ is presented. The mole fractions of $BF_3$ and MeCP used to prepare the solutions are $2.9 \times 10^{-4}$ and $1.8 \times 10^{-5}$, respectively. New bands due to complex formation are observed at 901.9 $cm^{-1}$ and at 891.7 $cm^{-1}$. The assignments in this region are not straightforward, neither for monomer MeCP nor for the complex. The observed contours impose that in the vapor phase $\nu_{23}^{MeCP}$ must be assigned on the high-frequency side of $\nu_{15}^{MeCP}$.[16] Yet the DFT calculations, Table 2, put $\nu_{15}^{MeCP}$ well above $\nu_{23}^{MeCP}$. Moreover, the resolution proposed for this doublet[16] indicates that $\nu_{23}^{MeCP}$ is much more intense than $\nu_{15}^{MeCP}$, contradicting the DFT intensities for these modes. Thus, it must be concluded that the DFT calculations fail to reproduce the details of the infrared spectrum in this region. This may be due to anharmonic influences on the experimental spectrum not accounted for in the calculations. The most straightforward procedure for assigning the monomer bands in Figure 5 would be to extrapolate the vapor phase order of assignment to the solutions. However, the much smaller intensity of the high-frequency component in LAr, in comparison with the vapor phase, is remarkable and casts some doubt on such extrapolated assignment. Next, the observed complex bands at 901.9 and 891.7 $cm^{-1}$ must be associated with the observed monomer bands. For this, it is tempting to take guidance from the relative intensities and associate the more intense complex band with the more intense monomer band. The above, however, shows that it cannot be excluded that the relative intensities change dramatically from vapor phase to LAr solution, which is an argument against taking such guidance. There is no reliable way of associating the complex bands with the monomer bands, and the assignment of the latter being uncertain, the complex bands observed in this region cannot be used to extract evidence for the structure of the complex present in solution.

In the spectra shown in Figure 5, an additional weak band due to a second complex can be seen at the lowest temperatures, at 912 $cm^{-1}$. This band shows the same temperature and concentration intensity dependence as the 1079 $cm^{-1}$ band discussed above, and consequently, is also assigned to a 1:2 complex.

An analysis similar to that performed for $\nu_3^{BF_3}$ was carried out for the C−H stretching region. Trace *a* in Figure 6 is the spectrum in this region recorded from a mixed solution containing mole fractions of MeCP and $BF_3$ equal to $3.6 \times 10^{-5}$ and $3.6 \times 10^{-4}$, respectively, and rescaled spectra of monomer MeCP and monomer $BF_3$ are shown as traces *b* and *c*. The difference spectrum obtained by subtracting *b* and *c* from *a*, is shown as trace *d*. In the latter, CH stretching bands due to the

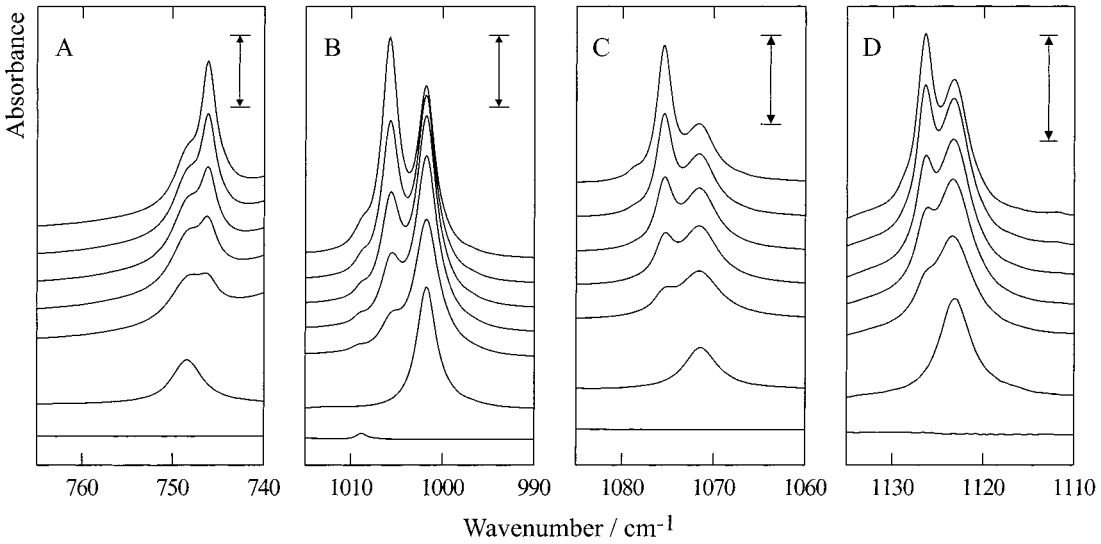


**Figure 4.** Infrared spectra of solutions in liquid argon. In each panel, the top five traces are recorded from a solution containing $BF_3$ and MeCP; from top to bottom the temperature increases from 110 to 126 K The lower two traces are recorded at 110 K from solutions containing only $BF_3$ and MeCP, respectively. A, region of $\nu_4^{MeCP}$; B, region of $\nu_7^{MeCP}$; C, region of $\nu_{14}^{MeCP}$; D, region of $\nu_{21}^{MeCP}$. The length of the vertical double arrow corresponds to an absorbance of 0.25.

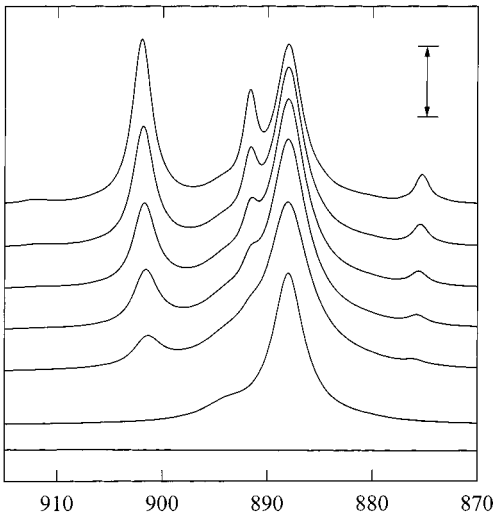


**Figure 5.** Infrared spectra of solutions in liquid argon in the region of $\nu_{15}^{MeCP}$ and $\nu_{23}^{MeCP}$. Top five traces: mixture of MeCP and $BF_3$; from top to bottom the temperature increases from 105 to 126 K. The lower two spectra are recorded at 107 K from solutions containing only MeCP and $BF_3$, respectively. The length of the vertical double arrow corresponds to an absorbance of 0.25.

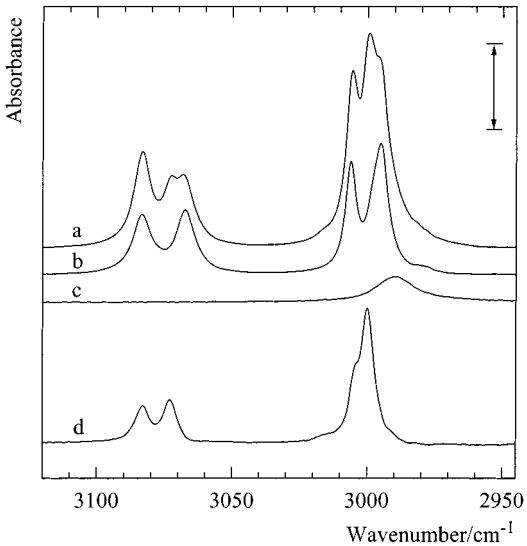


**Figure 6.** Infrared spectra of solutions in liquid argon in the CH stretching region, recorded at 106 K. a, Mixture of $BF_3$ and MeCP; b, solution containing only MeCP; c, solution containing only $BF_3$; d, difference spectrum resulting from the subtraction of traces b and c from a. The length of the vertical double arrow corresponds to an absorbance of 0.5.

complex are observed at 3083.2, 3072.8, 3006, and 2999.9 $cm^{-1}$. The highest of these, assigned as $\nu_{18}^{MeCP}$, is shifted by not more than $+0.5$ $cm^{-1}$ from the monomer position. The predictions in Table 2 for this mode range from $+2.4$ $cm^{-1}$ for isomer **I** to $+5.2$ $cm^{-1}$ for isomer **III**. Thus, although not quantitative, agreement is best with the predictions for isomer **I**. For the second band, at 3072.8 $cm^{-1}$, the experimental shift, $+5.2$ $cm^{-1}$, agrees well with that calculated for isomer **I** but disagrees with the shifts predicted for the other isomers.

We assign the 3000 $cm^{-1}$ doublet in the same order as for the monomer, i.e., the high-frequency component is assigned as $\nu_1^{MeCP}$ and the low-frequency one as $\nu_{19}^{MeCP}$, with $\nu_2^{MeCP}$ nearly accidentally degenerate, but not separetly detectable, with $\nu_{19}^{MeCP}$. Comparison with the corresponding monomer frequencies, 3006.1 and 2995.1 $cm^{-1}$, shows that the former is hardly affected by the complexation, whereas the latter is shifted by $+$ 4.8 $cm^{-1}$. Both shifts agree well with those predicted for isomer **I**, $-0.1$ and $+3.3$ $cm^{-1}$, respectively, whereas the agreement with the predictions for the other isomers is much poorer.

**C. Stoichiometry of the Observed Species.** The stoichiometry of the complex was determined in the manner previously described.[21] In this analysis, the band area of a complex band $I_c$ is plotted, for various integer values of $x$ and $y$, against $(I_{MeCP})^x \times (I_{BF3})^y$, in which $I_{MeCP}$ and $I_{BF3}$ are monomer band areas. For the present case, mixed solutions were investigated at 115 K, in which the MeCP mole fractions were varied between $1 \times 10^{-5}$ and $3 \times 10^{-4}$, and that of $BF_3$ between $3 \times 10^{-6}$ and $7 \times 10^{-4}$. For monomer MeCP and for the complex the band areas were obtained from a least squares band fitting, using Gauss/Lorentz sum functions, of the $2\nu_{15}^{MeCP}$ region, while for $BF_3$ the intensity of the $\nu_1^{BF_3} + \nu_3^{BF_3}$ combination band at 2375.4 $cm^{-1}$ was used. With these band areas, plots were prepared using 1 and 2 as values for $x$ and $y$. For each plot, a linear regression

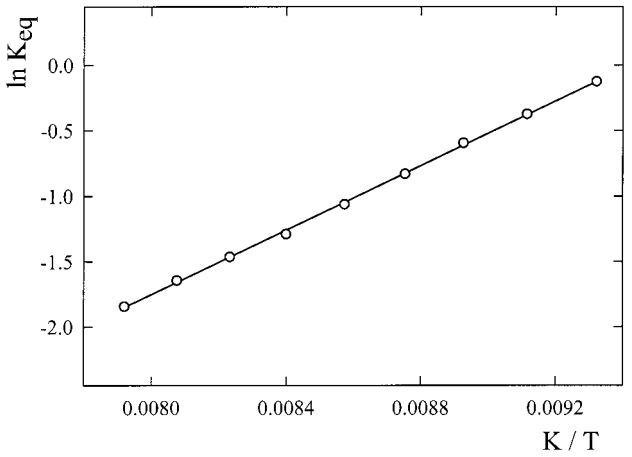


**Figure 7.** Van't Hoff plot for MeCP·$BF_3$.

was performed. The $\chi^2$-values for these regressions are 0.022 ($x = 1$; $y = 1$), 1.986 ($x = 1$; $y = 2$), 0.877 ($x = 2$; $y = 1$) and 2.906 ($x = 2$; $y = 2$). Thus, the best fit is obtained for $x = y = 1$. From this follows that the complex has a 1:1 stoichiometry.

**D. Complexation Enthalpy.** The complexation enthalpy $\Delta H_{LAr}^{o}$ for MeCP·$BF_3$ was derived from a van 't Hoff plot. The latter was constructed by plotting the logarithm of the ratio of band areas $I_{MeCP\cdot BF3}/(I_{MeCP} \times I_{BF3})$, measured at different temperatures, against the inverse temperature, $1/T$. The slope of this plot, corrected for thermal expansion of the solution,[22,23] equals $\Delta H_{LAr}^{o}/R$. For the present study, solutions containing mole fractions of $1.2 \times 10^{-4}$ in MeCP and $3.6 \times 10^{-4}$ in $BF_3$ were recorded at nine different temperatures between 107 and 127 K. The resulting van 't Hoff plot, obtained by using the band areas of the same monomer and complex bands as in the above concentration study, is shown in Figure 7. From the slope of the linear regression line, the complexation enthalpy $\Delta H_{LAr}^{o}$ for MeCP·$BF_3$ in liquid argon was calculated to be $-10.7(3)$ kJ $mol^{-1}$.

## Discussion

It is clear from the above that whenever the DFT calculations predict significantly different frequencies for the three possible isomer, the comparison with the bands observed in LAr directs the conclusion toward isomer **I**. This is regarded as sufficient evidence that in our solutions isomer **I** was formed. As no other 1:1 complex bands could be identified, the concentrations of isomers **II** and **III** must have been below the detection limit.

In addition to the bands due to MeCP·$BF_3$, in the spectra two weak bands, which we assign to a trimer species MeCP·$(BF_3)_2$, were observed. For the structure of this complex, several possibilities arise. First, it must be considered that MeCP binds to a $(BF_3)_2$ dimer. This species has been observed in matrixes, and its properties have been well described.[24−26] However, the $BF_3$ dimer has not yet been observed in cryosolutions, making this structure rather unlikely. A second possibility would be that one $BF_3$ binds to the double bond and the other to one of the pseudo-$\pi$ bonds of the ring. However, in view of the absence of isomers **II** and **III** in our study, this structure also is not very likely. In the third possible structure, both $BF_3$ molecules bind to the double bond, on opposite sides of the plane of the double bond. The plausibility of this structure was investigated using DFT calculations at the same level as for the 1:1 complexes. The resulting equilibrium geometry is shown in Figure 8. The complexation energy for this complex equals $-16.53$ kJ $mol^{-1}$. This value is somewhat less than twice the complexation energy of isomer **I**, which shows that the van der Waals bonds

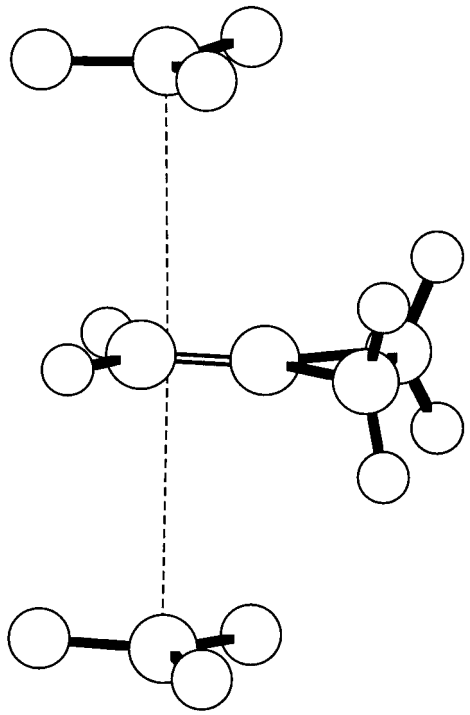

**Figure 8.** The proposed structure for MeCP·$(BF_3)_2$.

**TABLE 4. Observed and Calculated Vibrational Frequencies, in $cm^{-1}$, for MeCP·$(BF_3)_x$**

| | experimental | | | B3LYP/6-311++G(d,p) | | |
|---|---|---|---|---|---|---|
| mode | monomer | MeCP·$^{11}BF_3$ | MeCP·$(^{11}BF_3)_2$ | monomer | MeCP·$^{11}BF_3$ | MeCP·$(^{11}BF_3)_2$ |
| $\nu_{15}^{MeCP}$ | 888.0 | 901.9 | 912.1 | 920.0 | 923.7 | 944.3 |
| $\nu_{14}^{MeCP}$ | 1071.4 | 1075.5 | 1078.8 | 1094.0 | 1097.9 | 1099.1 |

in the 1:2 complex are slightly weaker than in isomer **I**. In Table 4, the observed frequencies for the species are compared with the values calculated. It can be seen that the agreement between the theoretical and the experimental shifts is very good, which adds to the likelihood of our proposed structure.

A quantity of interest for the complex is its complexation energy. It can be obtained from the complexation enthalpy in solution by correcting for solvation effects and for thermal and zero-point vibrational contributions. In this study, the Gibbs energy of solvation $\Delta G_{sol}$ for the monomers and for MeCP·$BF_3$ (**I**) were obtained from Monte Carlo calculations on the solutions, using Free Energy Perturbation Theory as included in BOSS 4.1.[27] The solvation enthalpy difference, $\Delta H_{sol}$, and solvation entropy difference, $\Delta S_{sol}$, were extracted using a finite difference method similar to the one described by Levy et al.[28] All of the intermolecular interactions were described using Lennard−Jones type functions, one for each pair of atoms. The parameters of these functions for the interaction of the C and H atoms with Ar were taken from the OPLS all-atom potential functions included in BOSS 4.1,[29] whereas those for the interaction of the B and F atoms with Ar were used as before.[30] The resulting solvation enthalpies and entropies are given in Table 5. From these, it follows that the complexation enthalpy in LAr is smaller than the vapor phase value by 3.34(39) kJ $mol^{-1}$. Correction of $\Delta H_{LAr}^{o}$ with this value results in a vapor phase complexation enthalpy $\Delta H_{vapor}^{o}$ of $-14.0(5)$ kJ $mol^{-1}$. In the next step, statistical thermodynamics[31] was applied to transform this value into an energy. For all of the species, the zero-point vibrational energies were calculated using B3LYP/6-311++G(d,p) DFT frequencies. The thermal contributions

**TABLE 5. Solvation Enthalpies, in kJ mol$^{-1}$, and Solvation Entropies, in J K$^{-1}$ mol$^{-1}$, Calculated Using Free Energy Perturbation Theory**

| species | $\Delta H_{sol}$ | $\Delta S_{sol}$ |
|---|---|---|
| $BF_3$ | −7.85 (15) | −26.98 (14) |
| MeCP | −24.95 (31) | −90.7 (26) |
| MeCP·$BF_3$ (isomer **I**) | −29.46 (18) | −108.3 (16) |

were calculated at the midpoint of the temperature interval in which $\Delta H_{LAr}^{o}$ was determined. Translational and rotational contributions were calculated in the classical limit, using, for the rotational contributions, the DFT rotational constants. Vibrational thermal contributions were calculated in the harmonic approximation using the same frequencies as for the zero-point corrections. These calculations result in a correction of −1.98 kJ mol$^{-1}$. Applying this to the $\Delta H_{vapor}^{o}$ yields an "experimental" complexation energy $\Delta E_{exp}$ of −16.0(10) kJ mol$^{-1}$. The uncertainty on this quantity was, somewhat arbitrarily, chosen to be twice the value for $\Delta H_{LAr}^{o}$, to account for the approximations made in transforming it to $\Delta E_{exp}$.

The B3LYP/6-311++G(d,p) complexation energy for isomer **I**, −9.0 kJ mol$^{-1}$, is significantly smaller than the "experimental" value of −16.0(10) kJ mol$^{-1}$. The correction of the theoretical value for basis set superposition error by the counterpoise method results in a value of −6.0 kJ mol$^{-1}$, which is even further away from the experimental value. This result for MeCP·$BF_3$ confirms earlier observations that at the B3LYP/6-311++G(d,p) level, the stability of weakly bound molecular complexes is often seriously underestimated.[4,32]

A more accurate value for the complexation energy was obtained by including dispersion interactions via second-order Moeller−Plesset perturbation theory.[33] For each species, starting from the DFT geometries, single point calculations were made at the MP2 = full/aug-cc-PVTZ level. The resulting complexation energies, obtained before and after correction for BSSE, are −28.24 and −12.87 kJ mol$^{-1}$, respectively. Clearly, the uncorrected complexation energy seriously overestimates the experimental value, whereas the corrected one is quite close. It should be noted, however, that even at the MP2 = full/aug-cc-PVTZ level, the BSSE corrected complexation energy still underestimates the experimental value by ca. 20%. This is in line with earlier results and is interpreted to mean that at the calculated level, the BSSE is slightly overcorrected by the counterpoise method.[32]

To obtain more information on the use of B3LYP/6-311++G(d,p) frequencies for comparison with cryosolution data, in Figure 9 we have plotted the predicted complexation shifts, in abscissa, against the corresponding experimental values, in ordinate. It can be seen that, with two exceptions, a good correlation is found. The exceptions are the C═C stretching fundamental $\nu_3^{MeCP}$, which is known to be disturbed by Fermi resonance,[16] and the $\nu_{15}^{MeCP}$ mode, the problems with which were discussed above. Also in Figure 9, are the linear regression line and the 99% confidence interval, obtained by using all data except those for $\nu_3^{MeCP}$ and $\nu_{15}^{MeCP}$, are shown. The constants of the linear regression $\Delta\nu_{exp} = a\ \Delta\nu_{calc} + b$ are $a = 0.97(6)$ and $b = -0.15(47)$ cm$^{-1}$, whereas the correlation coefficient equals 0.99. It is interesting to note that within the limits of uncertainty the regression line passes through the origin of the plot; this, evidently, is in agreement with expectation. Also, the value of the direction cosine is nearly equal to 1.0 confirming earlier observations[20] that the complexation shifts in LAr in general agree very well with theoretical calculations at the present level.

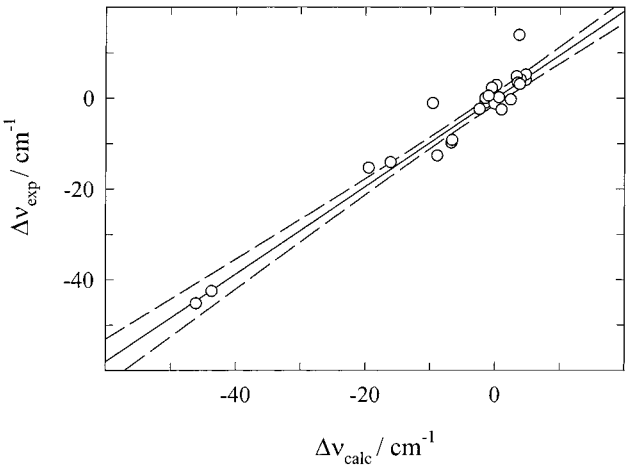


**Figure 9.** Comparison of the experimental complexation shifts of MeCP·$BF_3$, observed in liquid argon, in ordinate, with those calculated at the B3LYP/6-311++G(d,p) level, in abscissa. The linear regression line is drawn in full, the 99% confidence interval is delimited by the dashed lines.

**Acknowledgment.** W.A.H. thanks the Fund for Scientific Research (FWO-Vlaanderen) for an appointment as Postdoctoral Fellow. The FWO is also thanked for help toward the spectroscopic equipment used in this study. The authors thank the Flemish Community for financial support through the Bilateral Cooperation between Flanders and Poland.

**Supporting Information Available:** Table S1 reports B3LYP/6-311++G(d,p) equilibrium Cartesian coordinates for the 1:1 complexes of MeCP with $BF_3$. Table S2 compares the vibrational frequencies observed for MeCP in LAr at 100 K with the vapor phase frequencies and with the B3LYP/6-311++G(d,p) frequencies. This material is available free of charge via the Internet at http://pubs.acs.org.

## References and Notes

(1) Honeychuck, R. V. *J. Am. Chem. Soc.* **1989**, *111*, 6070.
(2) Yamamoto, Y. *Acc. Chem. Res.* **1987**, *20*, 243.
(3) Lewis, F. D.; Barancyck, S. V. *J. Am. Chem. Soc.* **1989**, *111*, 8653.
(4) Herrebout, W. A.; Van der Veken, B. J. *J. Am. Chem. Soc.* **1997**, *119*, 10 446.
(5) Everaert, G. P.; Herrebout, W. A.; Van der Veken, B. J.; Lundell, J.; Räsänen, M. *Chem. Eur. J.* **1998**, *4*, 321.
(6) Sass, C. E.; Ault, B. S. *J. Phys. Chem.* **1987**, *91*, 3207.
(7) Kisiel, Z.; Fowler, P. W.; Legon, A. C. *J. Chem. Phys.* **1994**, *101*, 4635.
(8) Kisiel, Z.; Fowler, P. W.; Legon, A. C. *Chem. Phys. Lett.* **1995**, *232*, 187.
(9) Legon, A. C.; Lister, D. G. *Phys. Chem. Chem. Phys.* **1999**, *1*, 4175.
(10) Sluyts, E. J.; Van der Veken, B. J. *J. Am. Chem. Soc.* **1996**, *118*, 440.
(11) Bertsev, V. V. Experimental technique. In *Molecular Cryospectroscopy*; Clark, R. J. H., Hester, R. E., Eds.; John Wiley & Sons: Chichester, 1995; pp 1−19.
(12) Frisch, M. J.; Trucks, G. W.; Schlegel, H. B.; Gill, P. M. W.; Johnson, B. G.; Robb, M. A.; Cheeseman, J. R.; Keith, T.; Petersson, G. A.; Montgomery, J. A.; Raghavachari, K.; Al-Laham, M. A.; Zakrzewski, V. G.; Ortiz, J. V.; Foresman, J. B.; Cioslowski, J.; Stefanov, B. B.; Nanayakkara, A.; Challacombe, M.; Peng, C. Y.; Ayala, P. Y.; Chen, W.; Wong, M. W.; Andres, J. L.; Replogle, E. S.; Gomperts, R.; Martin, R. L.; Fox, D. J.; Binkley, J. S.; Defrees, D. J.; Baker, J.; Stewart, J. P.; Head-Gordon, M.; Gonzalez, C.; Pople, J. A. Gaussian 94, Revision E4; Gaussian, Inc.: Pittsburgh, 1996.
(13) Becke, A. D. *J. Chem. Phys.* **1993**, *98*, 5648.
(14) Lee, C.; Yang, W.; Parr, R. G. *Phys. Rev. B* **1998**, *37*, 785.
(15) Boys, S. F.; Bernardi, F. *Mol. Phys.* **1970**, *19*, 553.
(16) Bertie, J. E.; Norton, M. G. *Can. J. Chem.* **1970**, *48*, 3889.
(17) Bertie, J. E.; Norton, M. G. *Can. J. Chem.* **1971**, *49*, 2229.
(18) Mitchell, R. W.; Merritt, J. A. *Spectrochim. Acta* **1971**, *27A*, 1609.

(19) Wurrey, C. J.; Nease, A. B. Vibrational spectroscopy and structure of three membered ring compounds. In *Vibrational Spectroscopy and Structure*; Durig, J. R., Ed.; Elsevier: Amsterdam, 1978; Vol. 7; p 32.
(20) Herrebout, W. A.; Van den Kerkhof, T.; Van der Veken, B. J. *J. Phys. Chem. A*, submitted for publication.
(21) Van der Veken, B. J.; De Munck, F. R. *J. Chem. Phys.* **1992**, *97*, 3060.
(22) Bertsev, V. V.; Golubev, N. S.; Shchepkin, D. N. *Opt. Spektrosk.* **1976**, *40*, 951.
(23) Van der Veken, B. J. *J. Phys. Chem.* **1996**, *100*, 17 436.
(24) Nxumalo, L. M.; Ford, T. A. *J. Mol. Struct.* **1993**, *300*, 325.
(25) Nxumalo, L. M.; Ford, T. A. *Vib. Spectrosc.* **1994**, *6*, 333.
(26) Nxumalo, L. M.; Ford, T. A. *J. Mol. Struct.* **1995**, *357*, 59.
(27) Jorgensen, W. L. BOSS 4.1; Yale University: New Haven, CT, 1999.
(28) Levy, R. M.; Gallicchio, E. *Annu. Rev. Phys. Chem.* **1998**, *49*, 531.
(29) Jorgensen, W. L.; Maxwell, D. S.; Tirado-Rives, J. *J. Am. Chem. Soc.* **1996**, *118*, 11 225.
(30) Herrebout, W. A.; Van der Veken, B. J. *J. Am. Chem. Soc.* **1998**, *120*, 9921.
(31) McQuarrie, D. A. *Statistical Mechanics*; Harper & Row: New York, 1976.
(32) Stolov, A. A.; Herrebout, W. A.; Van der Veken, B. J. *J. Am. Chem. Soc.* **1998**, *120*, 7310.
(33) Jensen, F. *Introduction to Computational Chemistry*; John Wiley & Sons: Chichester, 1999.